RSC Advances

PAPER

View Article Online
View Journal | View Issue

Cite this: *RSC Adv.*, 2017, **7**, 7567

Bi/AC modified with phosphoric acid as catalyst in the hydrochlorination of acetylene†

Di Hu, Feng Wang* and Jide Wang*

A series of H_3PO_4-modified Bi/AC catalysts with different P/Bi ratios were prepared by an incipient wetness impregnation method for the acetylene hydrochlorination reaction. The C_2H_2 conversion reduced in the following sequence: $BiP_{0.5}$/AC > BiP_1/AC > Bi/AC > $BiP_{0.1}$/AC > BiP_2/AC > BiP_3/AC. $BiP_{0.5}$/AC exhibited highest catalytic activity, with 82% conversion of C_2H_2 and 92% selectivity for vinyl chloride, among the catalysts that were investigated. Characterization was carried out using N_2 adsorption/desorption analysis, powder X-ray diffraction, transmission electron microscopy, thermogravimetric analysis, temperature-programmed reduction, atomic emission spectroscopy, and X-ray photoelectron spectroscopy. The results revealed that BiOCl was the main active species in the acetylene hydrochlorination reaction. The addition of H_3PO_4 promoted the dispersion of the Bi active component, strengthened the interaction between the metal and the support, and reduced the loss of the active component during the hydrochlorination of acetylene.

Received 15th November 2016
Accepted 9th January 2017

DOI: 10.1039/c6ra26845e

www.rsc.org/advances

Introduction

The hydrochlorination of acetylene is the most popular process in China for the production of vinyl chloride monomer (VCM), which is an irreplaceable raw material for the manufacture of polyvinyl chloride (PVC).[1–3] However, this process encounters challenges, such as environmental pollution and shortage of resources, owing to the use of activated-carbon-supported mercuric chloride ($HgCl_2$/C) catalysts.[4,5] Therefore, the desire to find a mercury-free catalyst, which is environmentally friendly for the PVC industry, has motivated much research activity.

In the past few decades, noble- and non-noble-metal catalysts have been employed for the hydrochlorination of acetylene.[1] Hutchings *et al.* investigated more than twenty types of metal components and concluded that their catalytic activity was correlated with the standard electrode potential of the metal cations.[6] Later, it was found that Au/C displayed high catalytic activity for the hydrochlorination of acetylene among a wide variety of investigated non-mercuric catalysts.[7,8] Recently, the addition of a second metallic component (Cu,[9–11] Co,[11,12] Cs,[13,14] K,[2] Ni,[15] Ba,[16] Bi,[17] *etc.*) to the Au/C catalyst and the modification of activated carbon with a reagent containing N,[18] P[19] or O[20] elements were studied. The results show that the dispersity, electronic structure of Au, and coke deposition rate were affected, as was the catalytic performance of the modified catalysts. However, Au/C catalysts still face hindrances owing to their high-cost and relatively short lifetime caused by the deposition of coke or the reduction of Au cations.[1] Non-noble-metal-based catalysts, which represent one of the important directions of development for the hydrochlorination of acetylene, have been extensively studied. According to the reports, bismuth-based catalysts exhibit better catalytic performance for the hydrochlorination of acetylene and are considered as a potential alternative to Hg-based catalysts. Wei *et al.* reported that a silica gel-supported Bi–Cu bimetallic catalyst has 30% of the activity of $HgCl_2$ and demonstrated the use of this catalyst in a 20-ton-per-year continuous fluidized-bed reactor for over 700 h, which represented a promising trial for the Hg-free chlor-alkali industry.[21] However, the role that the bismuth species play in the hydrochlorination reaction of acetylene and in the deactivation mechanism of Bi-based catalysts still remains unclear; thus, it needs to be further investigated.

BiOCl has a highly anisotropic structure and is attractive in many fields such as cosmetics, pharmaceuticals, battery cathodes, photocatalysis, and photoelectrochemical devices.[22] Doping with different types of semiconductors such as bismuth phosphates ($BiPO_4$),[23] graphitic carbon nitride (g-C_3N_4)[24] and bismuth sulfide (Bi_2S_3)[25] can improve the photocatalytic activity of BiOCl catalysts. Duo *et al.* found that $BiPO_4$/BiOCl composites exhibited much higher photocatalytic activity for the degradation of methyl orange than BiOCl and $BiPO_4$ alone under irradiation with simulated sunlight, owing to an effective increase in the speed of electron–hole separation during the photocatalytic process.[23] Shi *et al.* prepared a g-C_3N_4/BiOCl hybrid, which displayed superior performance for the photodegradation of rhodamine B in comparison with pure BiOCl under irradiation with visible light.[26] Also, it has been proven

Key Laboratory of Oil & Gas Fine Chemicals, Ministry of Education, Xinjiang University, Urumqi 830046, Xinjiang, People's Republic of China. E-mail: wangfeng62@126.com; awangjd@126.com

† Electronic supplementary information (ESI) available. See DOI: 10.1039/c6ra26845e

that $BiPO_4$ would exhibit activity in the hydrochlorination reaction of acetylene.

We are interested in studying whether or not a $BiPO_4$ additive can improve the catalytic performance of BiOCl-type catalyst for the hydrochlorination of acetylene. In this paper, a series of phosphorus-modified bismuth-based catalysts with varying molar ratios of P/Bi were prepared *via* an incipient wetness impregnation method using $BiCl_3$ and phosphoric acid as the precursors and coal-based carbon as the support. The catalytic properties were evaluated for the hydrochlorination of acetylene. In addition, the effects of the phosphorus content on the crystalline phases and dispersion of Bi species, as well as the structure of the catalysts, were also discussed and studied in detail.

Experimental

Catalyst preparation

Carbon-supported bismuth catalysts were prepared by an incipient wetness impregnation method using dilute aqueous hydrochloric acid (HCl; 2 mol L^{-1}). Coal-based activated carbon with a surface area of 878 m^2 g^{-1} measured by the BET method was selected as the catalyst support. Analytical-grade $BiCl_3$ and phosphoric acid were used as precursors of the metal and P. All the agents were used without any purification. The Bi loading content of each Bi-based catalyst was fixed at 16 wt%. At first, the metal precursor was dissolved in concentrated hydrochloric acid, and then the solution was diluted to a certain concentration. The support was added to the obtained solution under stirring. The mixture was treated under microwave irradiation for 1 h, after being set aside for 1 h. Then, the product was kept at room temperature for 8 h and finally dried at 120 °C in an oven for 8 h and used as a catalyst (which was designated as Bi/AC). In comparison with the preparation process of Bi/AC, the preparation procedure of Bi/AC catalysts modified with H_3PO_4 included the addition of a calculated amount of phosphoric acid to the metal precursor solution. The obtained sample was designated as BiP_X/AC, where X represents the molar ratio of P/Bi, which varied from 0.1 to 3.

Catalytic performance testing

Activity tests were carried out in a fixed-bed reactor equipped with a quartz tube microreactor (i.d. 10 mm) operating at a pressure of 0.1 MPa and a temperature of 160 °C. A N_2 flow (20 mL min^{-1}) regulated *via* calibrated mass flow controllers was first used to remove moisture and air in the system, and then hydrochloride at a flow rate of 15 mL min^{-1} was passed through the heated quartz tube reactor to activate the catalyst. After the reactor was heated to the target temperature, a gas flow that maintained a volume ratio of HCl : C_2H_2 of 1.25 : 1 and a total gas hourly space velocity (GHSV) of 120 h^{-1} was fed into it. The products from the reactor were absorbed with sodium hydroxide solution and then analyzed by a gas chromatograph (GC 2010, Shimadzu) equipped with a hydrogen flame ionization detector (FID) to determine the conversion of acetylene (X_A) and the selectivity for VCM (S_{VC}) immediately.

Catalyst characterization

The BET specific surface area (SSA) and pore structure information of the catalysts were investigated using a Quantachrome Autosorb automated gas sorption system. The surface areas of the catalysts were determined by the BET method, and the pore volume and average pore diameter were calculated by the BJH method applied to the desorption branches of the nitrogen isotherms.

X-ray diffraction (XRD) data were obtained using a M18XHF22-SRA diffractometer operating at 50 kV and 100 mA with Cu Kα radiation in the 2θ scan range between 10° and 80° (10° per min).

Transmission electron microscopy (TEM) was performed with a JEM-2100F instrument at an accelerating voltage of 200 kV. The samples were ground to a fine powder and dispersed in ethanol, and then one droplet of the ethanol suspension was placed and vaporized on a TEM grid with a 300 mesh copper and porous carbon film.

Thermogravimetric (TG) analysis was performed with a NETZSCH SAT 449F3 multifunctional thermal analyzer under an air atmosphere at a flow rate of 100 mL min^{-1}. The temperature was increased from 25 to 800 °C at a heating rate of 5 °C min^{-1}.

Temperature-programmed reduction (TPR) experiments were conducted using a TP-5080 adsorption instrument with a flow of hydrogen (7% in N_2) at a rate of 45 mL min^{-1}. The weight of the tested samples was about 50 mg. The temperature was increased from 20 to 800 °C at a rate of 10 °C min^{-1}. The consumption of hydrogen was measured using a thermal conductivity detector (TCD).

The surface elemental composition of the catalysts was determined by X-ray photoelectron spectroscopy (XPS) data acquired with a Kratos AXIS Ultra DLD spectrometer with a monochromatized aluminum X-ray source ($h\nu$ = 1486.6 eV), hybrid (magnetic/electrostatic) optics, a multichannel plate and a delay line detector (DLD). All XPS spectra were recorded using an aperture slot of 300 × 700 microns; survey spectra were recorded with a pass energy of 80 eV, and high-resolution spectra with a pass energy of 40 eV. The pressure in the sample analysis chamber was lower than 6×10^{-9} Torr during data acquisition.

The content of Bi in all samples was determined by inductively coupled plasma atomic emission spectroscopy (ICP-AES) analysis, which was carried out using a PerkinElmer Optima 8000 spectrometer.

Results and discussion

Catalytic performance in hydrochlorination of acetylene

The performance of Bi/AC and BiP_X/AC and the influence of the P content were first studied. In this section, P was introduced into the Bi/AC catalyst to improve the catalytic activity and a series of BiP_X/AC catalysts were tested, while the molar ratio of P/Bi was varied from 0.1 to 3. Fig. 1 shows the catalytic performance of the catalysts for the hydrochlorination of acetylene under the reaction conditions. For the Bi/AC catalyst, the

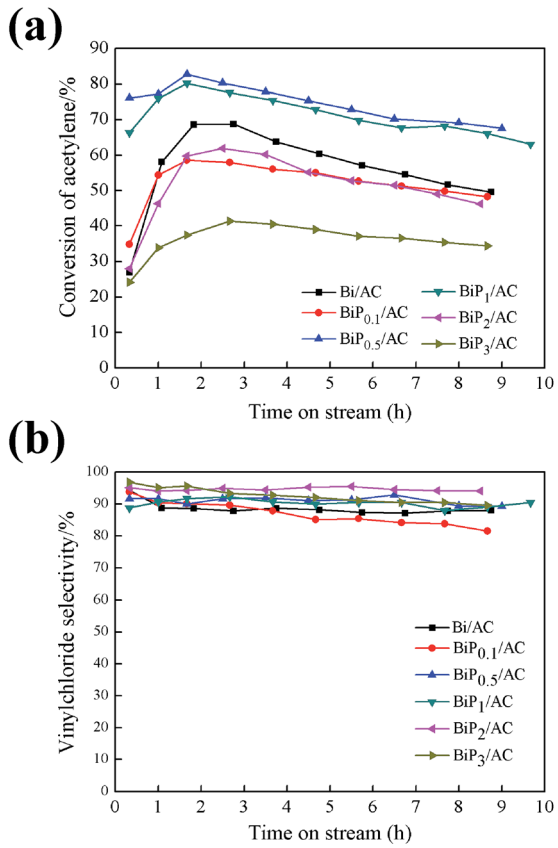

Fig. 1 Conversion of acetylene (a) and selectivity for VCM (b) over Bi/AC and BiP_X/AC catalysts. Reaction conditions: temperature (T) = 160 °C, GHSV = 120 h^{-1}, and feed volume ratio $V(HCl)/V(C_2H_2) = 1.25$.

conversion of acetylene reached 68.7% at first and then decreased to 49.6% at 9 h, *i.e.*, a reduction of about 30%. The selectivity for VCM was maintained at about 90% during the reaction time. For the modified BiP_X/AC catalysts, the catalytic performance and selectivity differed from each other with the P/Bi molar ratio. Among these, both the conversion of acetylene and the selectivity for VCM of the $BiP_{0.5}$/AC catalyst were higher than those of Bi/AC. The conversion of acetylene reached 82.8% and declined to 67.5% after the reaction had run for 9 h, *i.e.*, a reduction of about 18%. The results indicated that the H_3PO_4 additive can appropriately enhance the catalytic performance and stability of Bi-based catalysts for the hydrochlorination of acetylene.

Also, from Fig. 1 the effect of the P/Bi molar ratio on the performance of the Bi-based catalysts for the hydrochlorination reaction of acetylene was observed. Along with an increase in the phosphorus dopant content, the BiP_X/AC catalysts displayed volcano-type catalytic behavior on the basis of the conversion achieved by the catalysts. The catalysts with a lower (1 : 0.1) or higher (1 : 1, 1 : 2 and 1 : 3) H_3PO_4 content exhibited a decrease in the conversion of C_2H_2, the conversion of acetylene was 58.5%, 80.2%, 61.9%, and 41.4%, respectively, in comparison to the $BiP_{0.5}$/AC catalyst, for which the conversion of acetylene was 82.8%. Thus, on the basis of the performance in the catalytic experiments, it is indicated that the introduction of a suitable amount of H_3PO_4 into the catalyst significantly increased its activity in comparison to single-component Bi/AC. A smaller amount of the H_3PO_4 additive may impede the simultaneous formation of BiOCl particles, which resulted in further growth of crystals, and excessive amounts of the H_3PO_4 additive could block the pores, which is reflected by decreases in specific surface area from 288 $m^2\ g^{-1}$ to 55 $m^2\ g^{-1}$ and in pore volume from 0.18 $cm^3\ g^{-1}$ to 0.060 $cm^3\ g^{-1}$ (in Table 2), which resulted in a decline in active surface area and catalytic activity.

Fig. 2 shows the result of a 100 h catalytic performance test of $BiP_{0.5}$/AC under the conditions of GHSV(C_2H_2) = 30 h^{-1}, T = 160 °C, and $V(HCl)/V(C_2H_2) = 1.25$. It is indicated that the initial conversion of acetylene by the catalyst could reach 90%, and then the $BiP_{0.5}$/AC catalyst was deactivated gradually after achieving the highest conversion. However, the deactivation process was slowed significantly in comparison to the Bi/AC catalyst under the same conditions, but the $BiP_{0.5}$/AC catalyst was also deactivated rapidly in comparison to other types of catalyst, although it largely extended the lifetime of bismuth-based catalysts. It is therefore necessary to study the mechanisms of the improvement of Bi-based catalysts to obtain a theoretical foundation for future upgrades.

Characterization of catalysts

The Bi/AC and BiP_X/AC catalysts were characterized by XRD, TEM, TGA, TPR, XPS, ICP and BET analysis to study the effects of the H_3PO_4 additive on the structure and physicochemical properties of the bismuth catalysts.

The XRD patterns of the Bi/AC and BiP_X/AC catalysts are shown in Fig. 3. In the XRD pattern of Bi/AC, diffraction peaks characteristic of BiOCl at 2θ = 12.0°, 25.9°, 32.6°, 33.5°, 40.9°, 46.7°, 54.2° and 58.7° were observed. These peaks could be perfectly indexed to the (001), (101), (110), (102), (112), (200), (211), and (212) planes of tetragonal BiOCl (JCPDS 06-0249).[27] The peak at 2θ = 26.6° represents the (111) plane of graphitic carbon (JCPDS 75-2078). No diffraction peaks of other Bi species are observed, which indicates that BiOCl crystal particles were the active components in the Bi/AC catalyst.

After the addition of H_3PO_4, the characteristic patterns changed gradually with an increase in the P/Bi molar ratio in the range of 0.1–3. For the $BiP_{0.5}$/AC catalyst, the average particle size of BiOCl crystallites was smaller than for Bi/AC and $BiP_{0.1}$/AC, as a result of calculations of the BiOCl (101) diffraction peak using the Scherrer equation (see Table S1†). The quantity of $BiPO_4$ particles increased with an increase in the content of the H_3PO_4 additive. After the Bi/P molar ratio increased to 0.5, both BiOCl and $BiPO_4$ species were detectable and peaks at 2θ = 27.15°, 29.10° and 31.23° were observed, which suggested that a new $BiPO_4$ species was formed and the BiOCl crystallites began to diminish. When the Bi/P molar ratio was equal to 3.0, $BiPO_4$ species that contained three types of crystalline phase (LTMBIP, TBIP, and HTMBIP) were confirmed.[28]

Fig. 4 shows the XRD patterns of the fresh and used Bi/AC and $BiP_{0.5}$/AC catalysts. As can be seen, after reacting for a few hours under the reaction conditions the diffraction peaks of the used Bi/AC catalyst were smaller and fewer than those of fresh

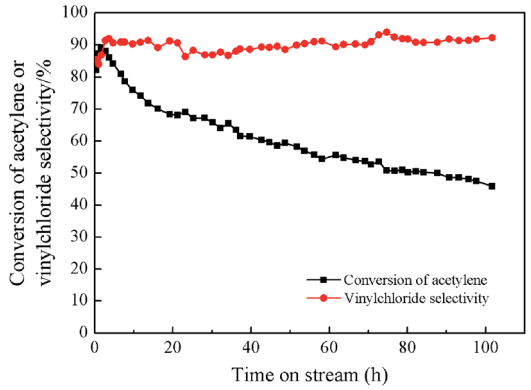

Fig. 2 Estimation of lifetime of $BiP_{0.5}$/AC catalyst. Reaction conditions: temperature (T) = 160 °C, GHSV(C_2H_2) = 30 h^{-1}, and feed volume ratio V(HCl)/V(C_2H_2) = 1.25.

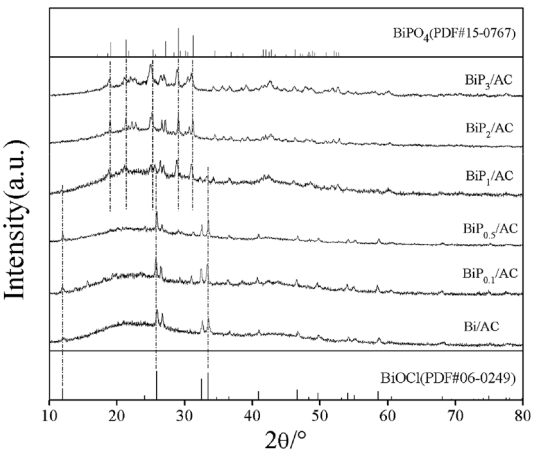

Fig. 3 XRD patterns of fresh Bi/AC and BiP_X/AC catalysts with varying H_3PO_4 contents.

Bi/AC, according to the following characteristic results, which may be caused by the loss of bismuth components or the formation of coke deposits on the surface. In used $BiP_{0.5}$/AC, the diffraction peaks of BiOCl could hardly been detected, which corresponds to the fact that the bismuth species of $BiP_{0.5}$/AC was still better dispersed than the single-component Bi/AC catalyst, which led to higher activity in the reaction. Therefore, it is inferred that the addition of H_3PO_4 promoted the dispersion of the Bi species during the preparation.

The TEM technique was employed to provide detailed images of bismuth species and was considered to be a suitable method for offering us accurate results. It was anticipated that modification with phosphorus may increase the distribution of bismuth species on the surface of coal-based activated carbon. Fig. 5 shows TEM images of the fresh and used Bi/AC (Fig. 5a and c) and $BiP_{0.5}$/AC (Fig. 5b and d) catalysts after reacting for 600 min. The TEM images of the fresh catalysts show that the addition of phosphoric acid could improve the dispersion of the bismuth species on the activated carbon. As shown in Fig. S2,† the average particle sizes of the active component in Bi/AC and $BiP_{0.5}$/AC were 36.2 nm and 32.5 nm, respectively. In addition,

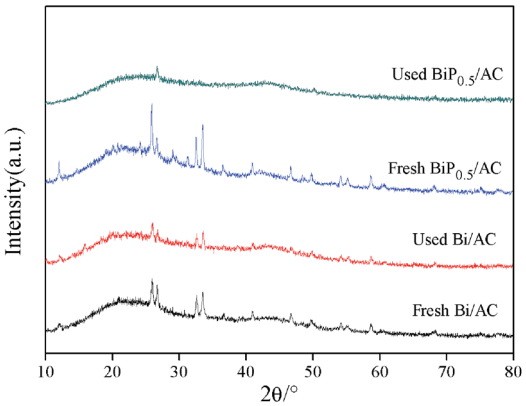

Fig. 4 XRD patterns of fresh and used Bi/AC and $BiP_{0.5}$/AC catalysts.

for the Bi/AC and $BiP_{0.5}$/AC catalysts the coverage density of black dots was clearly increased after the reaction, which indicates the aggregation of active species during the reaction time. Moreover, the particle sizes of nanoparticles in fresh and used $BiP_{0.5}$/AC were obviously smaller than in the Bi/AC samples. This phenomenon suggested that the growth of crystalline grains still occurred during the reaction but was restrained at the extremes of size. It was confirmed that the phosphorus species in the P-modified Bi-based catalyst can improve the dispersibility of bismuth element in the catalysts but also enhance the stability of bismuth ions during the hydrochlorination of acetylene.

We also selected two areas to investigate the nature of the active components in the catalysts. High-resolution TEM (HRTEM) images of the Bi/AC and $BiP_{0.5}$/AC catalysts are given in Fig. 6. Lattice fringes were clearly observed in the regions, which indicated that the bismuth components present in the catalysts were in a highly crystalline phase. The HRTEM image of Bi/AC (Fig. 6a) shows the resolved lattice spacing of 0.344 nm, which corresponds to the (101) plane of the tetragonal structure of BiOCl (JCPDS 06-0249).[27] As shown in Fig. 6b, the fringe spacing of 0.328 nm could be indexed to monoclinic $BiPO_4$ (JCPDS 15-0767),[28] whereas that of 0.344 nm corresponded well to the (101) plane of BiOCl. Therefore, it is very reasonable to state that BiOCl and $BiPO_4$ coexisted in the $BiP_{0.5}$/AC catalyst, which agrees with the results from the diffraction peaks that were found in XRD.

Temperature-programmed reduction (TPR) is a useful characterization technique for determining differences in the reducibility of the catalysts reported here, because it is able to provide information on the dimensions of the Bi particles and changes in the interactions between activated carbon and the supported substances.[15,18] Fig. 7 shows the TPR profiles of the AC, Bi/AC, $BiP_{0.1}$/AC, $BiP_{0.5}$/AC, BiP_1/AC, BiP_2/AC, and BiP_3/AC catalysts. For the Bi/AC sample, a characteristic reduction peak was exhibited in the range of 280–480 °C with its center at 438 °C, owing to the reduction of BiOCl species. There was also another peak at 541 °C, which was thought to be due to the reduction of carbon-containing functional groups such as carboxyl, phenol, ether, and lactone groups on the support surface.[29]

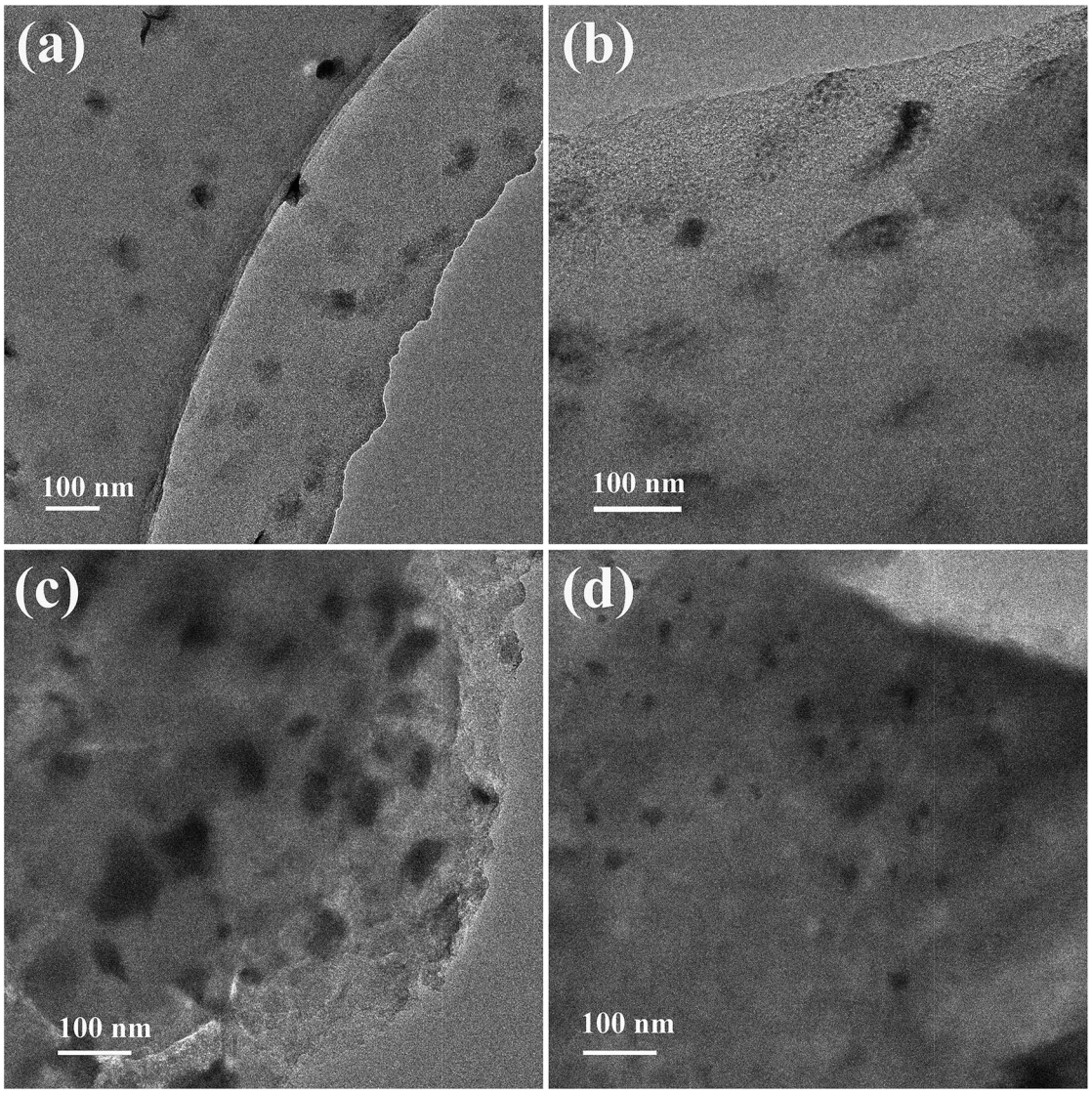

Fig. 5 TEM images of Bi/AC (a and c) and $BiP_{0.5}$/AC (b and d) before (a and b) and after (c and d) the reaction.

For the modified catalyst, as the Bi/P molar ratio increased in the range of 0.1–3 the reduction temperature of the Bi^{3+} peaks gradually divided into two, which indicated that two different types of Bi^{3+} species, namely, BiOCl and $BiPO_4$, coexisted in these catalysts. For the $BiP_{0.5}$/AC sample, a characteristic reduction peak that was centered around 406 °C was exhibited owing to the reduction of BiOCl species, which indicated that smaller Bi^{3+} particles were formed in $BiP_{0.5}$/AC that can provide more active sites to catalyze the hydrochlorination reaction of acetylene, which consequently resulted in high catalytic activity, in agreement with the results in Fig. 1. These findings suggest that the appropriate amount of the H_3PO_4 additive can promote the formation of the smaller BiOCl crystalline phase. When an excess amount of non-volatile H_3PO_4 was added, $BiPO_4$ species (peak centered around 520 °C) began to grow[30] and the strong interactions between the support and metal were enhanced as a result of the reduction temperature of $BiPO_4$ particles moving towards the high-temperature region. As this caused the formation of strong interactions, it would slow the loss of Bi^{3+}, which resulted in a deceleration in the deactivation rate. Catalysts doped with suitable amounts of H_3PO_4 display a significant decrease in the particle size of bismuth species, whereas the addition of extra phosphorus to the catalysts may change the active sites of the catalyst on the basis of the characteristic results of TPR, XRD and TEM. Therefore, Bi-based catalysts with various amounts of H_3PO_4 exhibited different catalytic performances. Thus, there was a strong correlation between the yield of VCM and the size of bismuth particles and species of active components in the catalyst.

The surface chemical compositions of the fresh and used catalysts were analyzed by XPS, and the results are shown in Fig. 8. The XPS survey spectrum (Fig. 8a) indicates that the as-prepared $BiP_{0.5}$/AC sample was composed of activated carbon and Bi^{3+} species, as shown by the strong peaks of C 1s, Bi 4f, Cl 2p, P 2p and O 1s. The presence of a P 2p peak in the spectrum shows that doping of P into the catalyst was successful. Fig. 8b

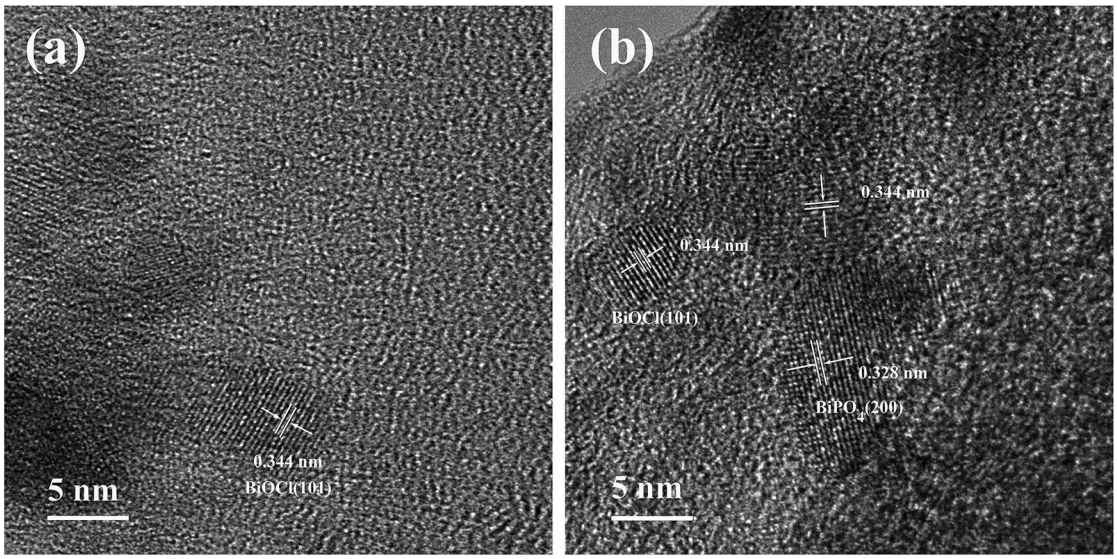

Fig. 6 HRTEM images of fresh Bi/AC (a) and $BiP_{0.5}$/AC (b).

shows the high-resolution XPS spectra of Bi 4f. The Bi $4f_{7/2}$ and Bi $4f_{5/2}$ peaks of Bi/AC are located at 159.9 and 165.2 eV (with a splitting energy of $\Delta = 5.3$ eV), which indicates that the Bi ions had a valence of +3.[17,31] Peaks attributed to the metallic state of Bi (at 156.4 and 161.6 eV) were not present in the spectrum of the catalyst, which indicated that in Bi/AC the active sites were Bi^{3+} species present in the form of BiOCl.[32] In the recent literature, reduction of the oxidation state of the active components to the metallic state of the metal leads to the deactivation of the catalyst for the reaction.[1] However, no obvious metallic state of Bi was detected for any of the used catalysts, which suggests that Bi^{3+} species may not have been reduced during the reaction time. Thus, the reduction of the active components may not be the main reason for the deactivation of Bi-based catalysts supported on activated carbon. Similar Bi 4f peaks were obtained for $BiP_{0.5}$/AC, and the binding energies of Bi 4f shifted to 159.7 eV and 165.1 eV, which were slightly lower than those in Bi/AC. On the other hand, the full width at half-maximum (FWHM) of the Bi 4f XPS peak became broader with an increase in the H_3PO_4 content (from 1.3 eV to 1.5 eV). This indicated the presence of smaller nanoparticles and PO_4^{3-}, which suggested an improvement in the dispersion of Bi into

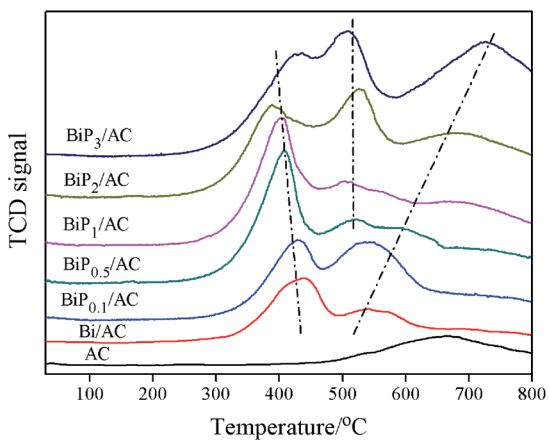

Fig. 7 H_2-TPR profiles of AC, fresh Bi/AC and BiP_X/AC.

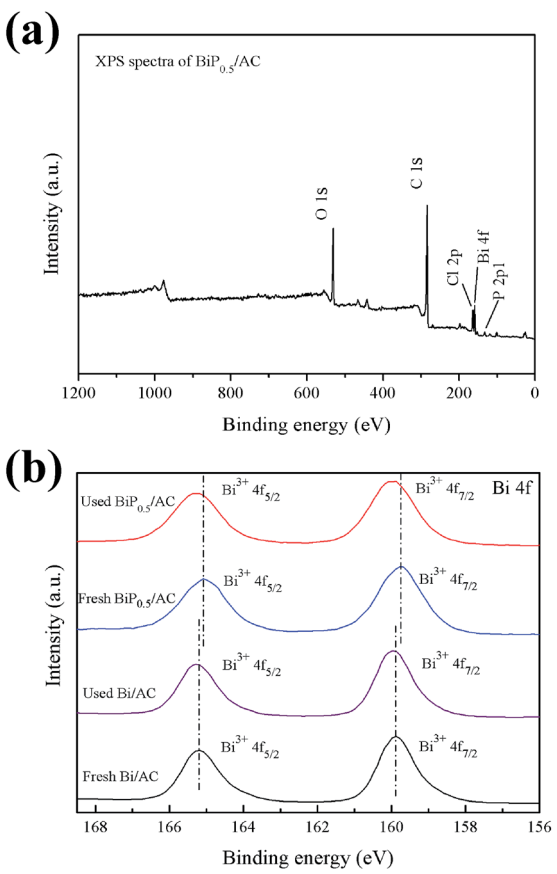

Fig. 8 (a) Wide-scan XPS spectrum of $BiP_{0.5}$/AC; (b) Bi 4f XPS spectra of fresh and used Bi/AC and $BiP_{0.5}$/AC.

tiny particles and changes in the chemical surroundings,[33,34] which consequently improved the catalytic performance for the hydrochlorination of acetylene.

In addition, the total Bi content in the fresh and used samples was also determined by ICP-AES, and the results obtained by XPS are also listed for comparison. As the results of ICP measurements show in Table 1, for the Bi/AC catalyst the loss ratio of Bi was 56.10% after the reaction, whereas for the $BiP_{0.5}$/AC catalyst the loss ratio was 16.46%, which suggests that the catalyst was much more stable after being doped with phosphorus. However, the Bi content calculated from XPS was relatively lower. Because the XPS technique mainly detects the contents of elements on the surface, this effect could be due to the fact that Bi particles preferred to occupy the inner space of the AC substrates. From the phenomenon that the total Bi content in the used catalysts was less than that in the fresh catalysts, it can be presumed that the loss of the active components was one of the main reasons that led to the deactivation of the catalysts, because the quantity of the active component that was lost was rather large in the used catalysts.

Low-temperature N_2 adsorption/desorption experiments were performed to investigate the physical structure of the Bi-based catalysts with the addition of H_3PO_4. The AC support alone displays a typical type I adsorption isotherm, because it contains a large number of micropores. For the Bi/AC and BiP_X/AC catalysts, similar adsorption isotherms are exhibited. As listed in Table 2, it could be seen that after loading the active bismuth species onto AC or adding the H_3PO_4 additive during the preparation process of Bi/AC the specific surface area and total pore volume of the Bi-based catalysts decreased, which was mainly due to the addition of the active components and the H_3PO_4 doping reagent. For Bi/AC, the specific surface area and total pore volume were 288 $m^2\ g^{-1}$ and 0.18 $cm^3\ g^{-1}$, respectively.

The conversion of C_2H_2 by the catalysts presented in the paper decreased in the following sequence: $BiP_{0.5}$/AC > BiP_1/AC > Bi/AC > $BiP_{0.1}$/AC > BiP_2/AC > BiP_3/AC, which was the same as the order of the specific surface areas of the fresh catalysts, which suggested that significant changes in textural structure in the pore structures after doping with H_3PO_4 were the main reasons that affected the initial conversion in the reaction. In addition, the specific surface area and total pore volume of the used catalysts were much lower than those of the fresh catalysts, which suggested that the reason for inactivation should be the formation of coke deposits resulting in pore blockage. After the reaction, the BET specific surface area and total pore volume of used Bi/AC decreased by 76.6% and 66.4% (10%), respectively; when H_3PO_4 was added, these two values changed to 88.2% and 73.5% (15%), respectively, which indicated that the deactivation of $BiP_{0.5}$/AC was mainly due to the formation of coke deposits, whereas the deactivation of Bi/AC was caused by the loss of the active components, which corresponded to the results of the ICP analysis.

Table S2† shows the specific activity per atom of bismuth ($B_{C_2H_2}{}^m$, $h^{-1}\ g^{-1}$ Bi) for the hydrochlorination of acetylene over

Table 1 Metal content derived from ICP and XPS measurements

Method	Catalyst	Total Bi (wt%) Fresh	Used	Loss ratio of Bi (%)
ICP	Bi/AC[a]	16.4	7.2	56.10
	$BiP_{0.5}$/AC[a]	15.8	13.2	16.46
Method	**Catalyst**	**Total Bi (atomic%) Fresh**	**Used**	**Loss ratio of Bi (%)**
XPS	Bi/AC[a]	1.92	0.86	55.21
	$BiP_{0.5}$/AC[a]	1.75	1.38	21.14

[a] Reaction conditions: GHSV = 120 h^{-1}, temperature (T) = 160 °C, feed volume ratio V(HCl)/V(C_2H_2) = 1.25, and reaction time: 10 h.

Table 2 Parameters of the porous structures of catalysts

Catalyst	S_{BET} ($m^2\ g^{-1}$) Fresh	Used	Total pore volume ($cm^3\ g^{-1}$) Fresh	Used
AC	878	—	0.53	—
Bi/AC	288	67	0.18	0.062
$BiP_{0.1}$/AC	93	57	0.10	0.078
$BiP_{0.5}$/AC	346	41	0.22	0.059
BiP_1/AC	315	33	0.21	0.050
BiP_2/AC	64	19	0.068	0.037
BiP_3/AC	55	30	0.060	0.046

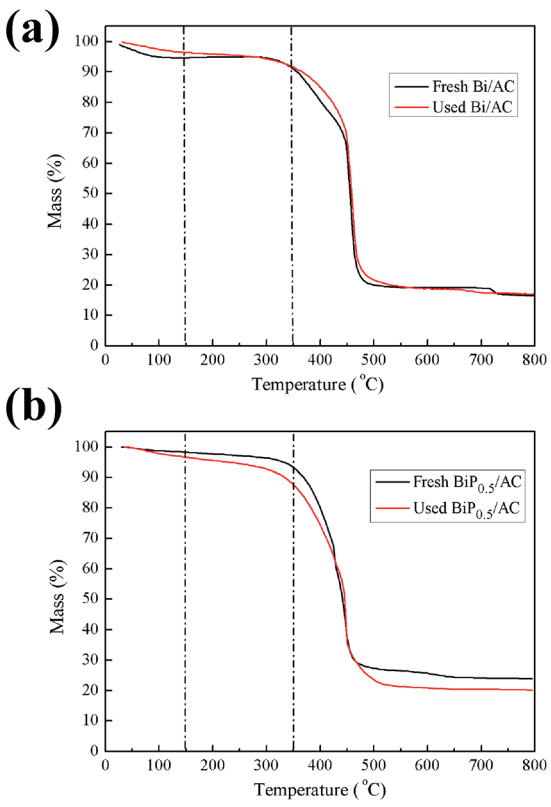

Fig. 9 TGA profiles of the fresh and used catalysts: (a) Bi/AC and (b) $BiP_{0.5}$/AC.

the catalysts at 160 °C (GHSV = 120 h^{-1}, feed volume ratio $V(HCl)/V(C_2H_2)$ = 1.25). In order to compare the intrinsic activity of the catalysts, the rate of conversion of C_2H_2 per square meter of catalyst ($B_{C_2H_2}{}^m$, h^{-1} g^{-1} cat.) was also listed according to the BET surface area to exclude the effect of dispersion on the activity. As can be seen, $BiP_{0.5}$/AC exhibited a higher $B_{C_2H_2}{}^m$ value than the remaining catalysts and displayed a more effective utilization factor of Bi atoms for the reaction, which indicated that an increase in the SSA affected the initial activity of the catalysts. In addition, surface chemical modification of the catalyst stabilized the Bi-based catalysts by suppressing the agglomeration of nanoparticles and reduced the loss of Bi components during the hydrochlorination of acetylene.

Thermogravimetric (TG) analysis is a typical method of achieving information on the deposition of coke on catalysts. However, in the case of catalysts supported on activated carbon the analysis is more intricate because activated carbon can react with oxygen to release CO and CO_2, which contributes to weight loss in the support. With the purpose of overcoming this difficulty, the amount of carbon deposited on the catalysts was determined on the basis of a calculation method reported before.[19] The TGA results show that neither the fresh nor the used Bi/AC catalyst displayed a significant loss of mass below 150 °C (Fig. 9a), which indicated that little adsorption of water occurred on the catalyst surface. In the range of 150–350 °C, the fresh Bi/AC catalyst exhibited a weight loss that reached 3.8%. When the temperature exceeded 400 °C, the catalyst rapidly decreased in weight because of the combustion of AC. On the other hand, the used Bi/AC catalyst exhibited a weight loss (4.8%) in the range of 150–350 °C, which was mainly due to the combustion of carbon deposited on the catalyst surface. With an increase in the P content, in comparison with the weight of coke deposits of 1.0% for used Bi/AC, the used $BiP_{0.5}$/AC catalyst after running for 10 h exhibited a larger decrease in weight of about 8.8% and the actual deposition of coke was 4.0% in the range of 150–350 °C. The BET results in Table 2 also provide indirect evidence of the problem of coke formation on the $BiP_{0.5}$/AC catalyst.

Conclusions

BiP_X/AC catalysts with different P/Bi molar ratios were prepared, and $BiP_{0.5}$/AC exhibited better catalytic performance than the Bi/AC catalyst. The optimum molar ratio of Bi/P was 1 : 0.5. The difference in activity could mainly be attributed to differences in the accessible surface areas of Bi. Characterizations of $BiP_{0.5}$/AC by ICP, BET, XRD, TEM, TG, H_2-TPR and XPS revealed that the addition of H_3PO_4 led to the formation of smaller crystalline particles, which resulted in an increase in catalytic activity. The addition of the P component allowed catalysts to be prepared with smaller BiOCl particles dispersed on the catalyst surface, suppressed the aggregation of Bi nanoparticles and reduced the loss of the active component during the hydrochlorination of acetylene. Catalytic tests of the hydrochlorination of acetylene showed a modest increase in activity to yield vinyl chloride when the P/Bi mole ratio was in the range of 0.5 to 1, whereas the catalytic activity could be further decreased upon an increase in the weight ratio from 1 to 3 owing to the formation of fewer active $BiPO_4$ particles and the blockage of pores. These new findings open an avenue for the rational design and bottom-up synthesis of low-cost highly active catalysts for the hydrochlorination of acetylene.

Acknowledgements

This work was supported by the Natural Scientific Foundation of China (Grant No. U1403293 and 21263025) and the Graduate Research and Innovation Program of Xinjiang (Grant No. XJGRI2015010).

References

1 M. Zhu, Q. Wang, K. Chen, Y. Wang, C. Huang, H. Dai, F. Yu, L. Kang and B. Dai, *ACS Catal.*, 2015, **5**, 5306–5316.
2 K. Zhou, J. Jia, C. Li, H. Xu, J. Zhou, G. Luo and F. Wei, *Green Chem.*, 2015, **17**, 356–364.
3 S. Chao, Q. Guan and W. Li, *J. Catal.*, 2015, **330**, 273–279.
4 S. Wang, B. Shen and Q. Song, *Catal. Lett.*, 2010, **134**, 102–109.
5 G. Deng, B. Wu, T. Li, G. Liu, L. Wang, W. Zhou and R. Chen, *Polyvinyl Chloride*, 1994, 5–9.
6 G. Hutchings, *J. Catal.*, 1985, **96**, 292–295.
7 M. Conte, A. F. Carley, G. Attard, A. A. Herzing, C. J. Kiely and G. J. Hutchings, *J. Catal.*, 2008, **257**, 190–198.
8 P. Johnston, N. Carthey and G. J. Hutchings, *J. Am. Chem. Soc.*, 2015, **137**, 14548–14557.
9 H. Xu, K. Zhou, J. Si, C. Li and G. Luo, *Catal. Sci. Technol.*, 2016, **6**, 1357–1366.
10 J. Zhao, J. Zeng, X. Cheng, L. Wang, H. Yang and B. Shen, *RSC Adv.*, 2015, **5**, 16727–16734.
11 H. Zhang, B. Dai, W. Li, X. Wang, J. Zhang, M. Zhu and J. Gu, *J. Catal.*, 2014, **316**, 141–148.
12 H. Zhang, B. Dai, X. Wang, W. Li, Y. Han, J. Gu and J. Zhang, *Green Chem.*, 2013, **15**, 829–836.
13 J. Zhao, T. Zhang, X. Di, J. Xu, S. Gu, Q. Zhang, J. Ni and X. Li, *Catal. Sci. Technol.*, 2015, **5**, 4973–4984.
14 J. Zhao, J. Xu, J. Xu, J. Ni, T. Zhang, X. Xu and X. Li, *ChemPlusChem*, 2015, **80**, 196–201.
15 Y. Pu, J. Zhang, X. Wang, H. Zhang, L. Yu, Y. Dong and W. Li, *Catal. Sci. Technol.*, 2014, **4**, 4426–4432.
16 H. Zhang, W. Li, X. Li, W. Zhao, J. Gu, X. Qi, Y. Dong, B. Dai and J. Zhang, *Catal. Sci. Technol.*, 2015, **5**, 1870–1877.
17 K. Zhou, W. Wang, Z. Zhao, G. Luo, J. T. Miller, M. S. Wong and F. Wei, *ACS Catal.*, 2014, **4**, 3112–3116.
18 J. Zhao, J. Xu, J. Xu, T. Zhang, X. Di, J. Ni and X. Li, *Chem. Eng. J.*, 2015, **262**, 1152–1160.
19 B. Wang, L. Yu, J. Zhang, Y. Pu, H. Zhang and W. Li, *RSC Adv.*, 2014, **4**, 15877–15885.
20 X. Cheng, J. Zhao, L. Wang, R. Ren, H. Yang and B. Shen, *Chin. J. Chem.*, 2014, **35**, 582–588.
21 K. Zhou, J. Jia, X. Li, X. Pang, C. Li, J. Zhou, G. Luo and F. Wei, *Fuel Process. Technol.*, 2013, **108**, 12–18.

22 H. Peng, C. K. Chan, S. Meister, X. Zhang and Y. Cui, *Chem. Mater.*, 2009, **21**, 247–252.
23 F. Duo, Y. Wang, X. Mao, X. Zhang, Y. Wang and C. Fan, *Appl. Surf. Sci.*, 2015, **340**, 35–42.
24 S. Hu, L. Ma, J. You, F. Li, Z. Fan, F. Wang, D. Liu and J. Gui, *RSC Adv.*, 2014, **4**, 21657–21663.
25 H. Cheng, B. Huang, X. Qin, X. Zhang and Y. Dai, *Chem. Commun.*, 2012, **48**, 97–99.
26 S. Shi, M. Gondal, A. Al-Saadi, R. Fajgar, J. Kupcik, X. Chang, K. Shen, Q. Xu and Z. Seddigi, *J. Colloid Interface Sci.*, 2014, **416**, 212–219.
27 S. Cao, C. Guo, Y. Lv, Y. Guo and Q. Liu, *Nanotechnology*, 2009, **20**, 1–7.
28 X. Wei, F. Wei, W. Jian, G. luo, H. Shi and Y. Jin, *Chin. J. Process Eng.*, 2008, **8**, 1218–1222.
29 G. Li, W. Li and J. Zhang, *Catal. Sci. Technol.*, 2016, **6**, 1821–1828.
30 Y. Lv, Y. Liu, Y. Zhu and Y. Zhu, *J. Mater. Chem. A*, 2014, **2**, 1174–1182.
31 N. Myung, S. Ham, S. Choi, Y. Chae, W. Kim, Y. Jeon, K. Paeng, W. Chanmanee, N. Tacconi and K. Rajeshwar, *J. Phys. Chem. C*, 2011, **115**, 7793–7800.
32 J. Grunwaldt, M. Wildberger, T. Mallat and A. Baiker, *J. Catal.*, 1998, **177**, 53–59.
33 J. Yu, B. Yang and B. Cheng, *Nanoscale*, 2012, **4**, 2670–2677.
34 H. Shin, H. Choi, Y. Jung, S. Kim, H. Song and H. Shin, *Chem. Phys. Lett.*, 2004, **383**, 418–422.